fractal and fractional

Article

Dynamical Behaviors of an SIR Epidemic Model with Discrete Time

Bo Li [1,2,*,†], Zohreh Eskandari [3,†] and Zakieh Avazzadeh [4,†]

1 Business School, Nanjing University, Nanjing 210024, China
2 School of Finance, Anhui University of Finance & Economics, Bengbu 233000, China
3 Department of Mathematics, Faculty of Science, Fasa University, Fasa 7461686131, Iran
4 Department of Mathematical Sciences, University of South Africa, Florida 0003, South Africa
* Correspondence: libomaths@163.com or libo@aufe.edu.cn
† These authors contributed equally to this work.

Abstract: Analytically and numerically, the study examines the stability and local bifurcations of a discrete-time SIR epidemic model. For this model, a number of bifurcations are studied, including the transcritical, flip bifurcations, Neimark–Sacker bifurcations, and strong resonances. These bifurcations are checked, and their non-degeneracy conditions are determined by using the normal form technique (computing of critical normal form coefficients). We use the MATLAB toolbox MATCONTM, which is based on the numerical continuation method, to confirm the obtained analytical results and specify more complex behaviors of the model. Numerical simulation is employed to present a closed invariant curve emerging from a Neimark–Sacker point and its breaking down to several closed invariant curves and eventually giving rise to a chaotic strange attractor by increasing the bifurcation parameter.

Keywords: SIR epidemic model; bifurcation; normal form; continuation method; strong resonances

Citation: Li, B; Eskandari, Z.; Avazzadeh, Z. Dynamical Behaviors of an SIR Epidemic Model with Discrete Time. *Fractal Fract.* **2022**, *6*, 659. https://doi.org/10.3390/fractalfract6110659

Academic Editors: Ravi P. Agarwal and Maria Alessandra Ragusa

Received: 8 October 2022
Accepted: 4 November 2022
Published: 7 November 2022

1. Introduction

There is a great deal that can be done to minimize the impact of infectious diseases through research. With relevant knowledge about the dynamics of an infection, disease transmission can often be prevented. The transmission and dynamics of most infectious diseases are greatly influenced by seasonal factors, including climatic factors and human phenomena [1]. It appears that intense seasonality causes erratic patterns based on some empirical data. The presence of chaotic oscillations in response to seasonal forces has been demonstrated in many studies focusing on seasonal influenza and measles [2,3]. When vaccination programs are not in place, many recurrent infectious diseases exhibit strong annual, biennial, or irregular oscillations in response to seasonality [4].

A mathematical model called the SIR allows us to estimate the number of people infected with a disease in a closed population over time. Susceptibility, infection, and recovery models are included in the SIR group.

The behavior of epidemic diseases is being studied in an effort to detect and control them. One of them is the dynamical epidemic model, which is used to study epidemics [5–14]. The dynamical nature of the measles epidemic model is analyzed in [14], and the dynamical nature of the disease is also strongly influenced by migration processes. The study in [15] demonstrated that chickenpox prevalence is inversely related to the size of the population on an annual cycle.

The mathematical modeling of infectious diseases leads to detect the dynamical behavior of epidemics and provide sufficient disease control measures. The treatment of epidemics is studied using a dynamic model [5–9]. An SIR (Sensitive–Infected–Improved) model has been used to study the dynamics of the measles epidemic [14]. According to research, the disease is very sensitive to migration, and its onset was accompanied by an epidemic. Based on [15], chickenpox prevalence is inversely proportional to population size on an annual cycle. In this paper, we aim to analyze model (3) for different types of bifurcations. The novelty of our work is that we studied the bifurcation results of discrete-time SIR epidemic model [1,4,16,17], as none of the studies in the literature has studied the complex dynamic behavior of the model.

According to classical infectious disease transmission models (Kermack and McKendrick [18], Hethcote [19]), the population is divided into three classes derived from $S(\iota)$, $I(\iota)$, and $R(\iota)$ indicating the number of susceptibles, infected individuals, and recovered or removed individuals at time ι, respectively. Here, we develop a model of SIR epidemics based on a modified saturated incidence rate as follows:

$$\begin{cases} \frac{dS}{d\iota} = \Lambda - \frac{\beta S(\iota) I(\iota)}{1+\alpha S(\iota)} - \delta S(\iota), \\ \frac{dI}{d\iota} = \frac{\beta S(\iota) I(\iota)}{1+\alpha S(\iota)} - (\delta + \sigma) I(\iota), \\ \frac{dR}{d\iota} = \sigma I(\iota) - \delta R(\iota), \end{cases} \tag{1}$$

where the saturated contact rate is indicated by $\frac{\beta S(\iota) I(\iota)}{1+\alpha S(\iota)}$ and more information about parameters can be found in Table 1.

Table 1. Description of parameters.

Parameter	Description
δ	Incidence of natural death in the population
β	Rate of incident bilinearity
Λ	Population recruitment rate
σ	Infection rate of infected individuals
α	Disease-induced death rate

Model (1) focuses on the following model because the first two equations are not dependent on R; see [20,21]:

$$\begin{cases} \frac{dS}{d\iota} = \Lambda - \frac{\beta S(\iota) I(\iota)}{1+\alpha S(\iota)} - \delta S(\iota), \\ \frac{dI}{d\iota} = \frac{\beta S(\iota) I(\iota)}{1+\alpha S(\iota)} - (\delta + \sigma) I(\iota). \end{cases} \tag{2}$$

Euler's method is applied to (2) to obtain the following discrete time model:

$$\begin{cases} S \mapsto S + h\left(\Lambda - \frac{\beta S I}{1+\alpha S} - \delta S\right), \\ I \mapsto I + h\left(\frac{\beta S I}{1+\alpha S} - (\delta + \sigma) I\right), \end{cases} \tag{3}$$

where h is step size.

2. Stability of Fixed Points

First, we present a lemma that describes the dynamics of the model (1).

Lemma 1. *In the first quadrant, the plane $S + I + R = \frac{\Lambda}{\delta}$ is an invariant manifold of the system of the model* (1).

Proof. When we combine the three equations in (1) and denote $N(\tau) = S(\tau) + I(\tau) + R(\tau)$, we obtain

$$\frac{dN}{d\tau} = \Lambda - \delta N.$$

For any $N(\tau_0) \geq 0$,

$$N(\tau) = \frac{1}{\delta}\Big[\Lambda - (\Lambda - \delta\, N(\tau_0))e^{-\delta\,(\tau-\tau_0)}\Big].$$

is the general solution. So, we have

$$\lim_{\tau\to+\infty} N(\tau) = \frac{\Lambda}{\delta},$$

the result can be drawn from this. □

There are two fixed points for model (3) as follows:

$$\mathcal{E}_0 = \left(\frac{\Lambda}{\delta}, 0\right), \quad \mathcal{E}_* = \left(-\frac{\delta+\sigma}{\alpha\,\delta + \alpha\,\sigma - \beta}, \frac{\Lambda\,\alpha\,\delta + \Lambda\,\alpha\,\sigma - \Lambda\,\beta + \delta^2 + \delta\,\sigma}{\alpha\,\delta^2 + 2\,\alpha\,\delta\,\sigma + \alpha\,\sigma^2 - \beta\,\delta - \beta\,\sigma}\right).$$

The fixed point $\mathcal{E}_*$ exists when $\mathcal{R}_0 > 1$, where $\mathcal{R}_0 = \frac{\Lambda\,\beta}{(\sigma+\delta)(\alpha\Lambda+1)}$.

Assign

$$\mathcal{A}_0 = \begin{pmatrix} -\delta\,h + 1 & -\frac{h\beta\,\Lambda}{\Lambda\,\alpha+\delta} \\ 0 & \frac{(-h\alpha\,\delta + (-\alpha\,\sigma+\beta)h+\alpha)\Lambda - \delta^2 h - \delta\,h\sigma + \delta}{\Lambda\,\alpha+\delta} \end{pmatrix},$$

and

$$\mathcal{A}_* = \begin{pmatrix} \frac{\left(-\Lambda\,(\delta+\sigma)^2\alpha^2 + (2\,\delta+2\,\sigma)\left(\Lambda\,\beta - 1/2\,\delta^2 - 1/2\,\delta\,\sigma\right)\alpha - \beta^2\Lambda\right)h + \beta\,(\delta+\sigma)}{\beta\,(\delta+\sigma)} & -h(\delta+\sigma) \\ \frac{h((-\delta-\sigma)\alpha+\beta)\left(-\Lambda\,\alpha\,(\delta+\sigma) + \Lambda\,\beta - \delta^2 - \delta\,\sigma\right)}{\beta\,(\delta+\sigma)} & 1 \end{pmatrix},$$

can be selected as the Jacobian matrix of (3) at $\mathcal{E}_0$ and $\mathcal{E}_*$

Theorem 1. *If $R_0 < 1$, the fixed point $\mathcal{E}_0$ is asymptotically stable when $-\frac{\delta\,(\delta+\sigma)}{\alpha\,\delta+\alpha\,\sigma-\beta} < \Lambda < -\frac{\delta\,(\delta\,h+h\sigma-2)}{\alpha\,\delta\,h+\alpha\,h\sigma-\beta\,h-2\,\alpha}$, provided that $0 < h < \frac{2}{\delta}$.*

Proof. See [22,23]. □

Theorem 2. *In the following cases, $\mathcal{E}_*$ is asymptotically stable:*

1. *If $\Delta_* > 0$ and $0 < \Lambda < \frac{\left(-h\delta\,(\delta+\sigma)(\delta\,h+h\sigma-2)\alpha+\beta\left(\delta^2h^2+\delta\,h^2\sigma-4\right)\right)(\delta+\sigma)}{(\delta\,h+h\sigma-2)((-\delta-\sigma)\alpha+\beta)^2 h}$,*
2. *If $\Delta_*^{SIR} < 0$ and $0 < \Lambda < \frac{(\delta+\sigma)^2((-\delta\,h-h\sigma+1)\alpha+\beta\,h)\delta}{(\delta\,h+h\sigma-1)((-\delta-\sigma)\alpha+\beta)^2}$,*

where $\Delta_* = \frac{\Delta_*^1}{\beta^2(\delta+\sigma)^2}$, and see more information for Δ_*^1 in Appendix A.

Proof. See [22,23]. □

3. Bifurcation Analysis of the Boundary FIXED Point $\mathcal{E}_0$

Our goal in this part is to investigate the bifurcations of model (3) at the trivial fixed point $\mathcal{E}_0$ by computing corresponding critical normal form coefficients; see [24–26].

In this section, the parameter Λ is considered as a bifurcation parameter.

Theorem 3. *The critical value $\Lambda_{LP,0} = \frac{\delta\,(\delta+\sigma)}{\beta-\alpha(\delta+\sigma)}$ causes a transcritical bifurcation of $\mathcal{E}_0$.*

Proof. For $\Lambda = \Lambda_{LP}$, $\mathcal{A}_0$ has the following multipliers:

$$\lambda_1^{LP,0} = +1, \qquad \lambda_2^{LP,0} = -\delta\, h + 1.$$

When $h \neq \frac{2}{\delta}$, the Jacobian matrix $\mathcal{A}_0$ has a single multiplier $+1$ and no other multiplier with $|\lambda| = 1$. So, the model (3) at $\beta = \beta_{LP,0}$ can be reduced to its normal form

$$\omega_{LP,0} \mapsto \omega_{LP,0} + \varphi_{LP,0}\omega_{LP,0}^2 + \mathcal{O}(\omega_{LP,0}^3),$$

where

$$\varphi_{LP,0} = -\frac{h((-\delta-\sigma)\alpha+\beta)^2(\delta+\sigma)}{\beta\,\delta}.$$

$\mathcal{E}_0$ develops a transcritical bifurcation because it is always the fixed point and will never disappear, and $\varphi_{LP,0} \neq 0$. □

Theorem 4. *The critical value* $\Lambda = \Lambda_{PD,0} = \frac{\delta\,(\delta h+\sigma h-2)}{2\,\alpha+h(\beta-\alpha\delta-\alpha\sigma)}$ *causes a flip bifurcation of* $\mathcal{E}_0$.

Proof. For $\Lambda = \Lambda_{PD,0}$, $\mathcal{A}_0$ has the following eigenvalues:

$$\lambda_1^{PD,0} = -1, \qquad \lambda_2^{PD,0} = -\delta\, h + 1.$$

When $\lambda_2^{PD,0} \neq \pm 1$, the Jacobian matrix $\mathcal{A}_0$ has a single multiplier -1 and no other multiplier with $|\lambda| = 1$. So, the model (3) at $\Lambda = \Lambda_{PD,0}$ can be reduced to its normal form

$$\omega_{PD,0} \mapsto -\omega_{PD,0} + \phi_{PD,0}\omega_{PD,0}^3 + \mathcal{O}(\omega_{PD,0}^4),$$

where

$$\phi_{PD,0} = \frac{\phi_{PD,0}^1}{\beta^2 h^2 (h\delta-2)^2\delta},$$

and

$$\phi_{PD,0}^1 = (h\delta+h\sigma-2)(\alpha\,\delta\,h+\alpha\,h\sigma-\beta\,h-2\,\alpha)^3\Big(\alpha\,\delta^3 h^2+2\,\alpha\,\delta^2 h^2\sigma+\alpha\,\delta\,h^2\sigma^2-\beta\,\delta^2 h^2$$
$$-\beta\,\delta\,h^2\sigma-3\,\alpha\,\delta^2 h-4\,\alpha\,\delta\,h\sigma-\alpha\,h\sigma^2+2\,\beta\,\delta\,h+\beta\,h\sigma+2\,\alpha\,\delta+2\,\alpha\,\sigma\Big).$$

As long as $\phi_{PD,0} > 0$ ($\phi_{PD,0} < 0$), the flip bifurcation is super-critical (sub-critical, resp.); moreover, the two-period emerging cycle is stable (unstable, resp.). □

4. Bifurcation Analysis of the Positive Fixed Point $\mathcal{E}_*$

Based on the equations given in [24–26], we will determine the critical normal form coefficient at the bifurcation points of the model (3).

4.1. One Parameter Bifurcations

Λ is referred to as a bifurcation parameter.

Theorem 5. *The presence of*

$$\Lambda = \Lambda_{PD,*} = \frac{\left(-h\delta\,(\delta+\sigma)(\delta\,h+h\sigma-2)\alpha+\beta\left(\delta^2 h^2+\delta\,h^2\sigma-4\right)\right)(\delta+\sigma)}{h((-\delta-\sigma)\alpha+\beta)^2(\delta\,h+h\sigma-2)},$$

causes a flip bifurcation of $\mathcal{E}_*$.

Proof. For $\Lambda = \Lambda_{PD,*}$, $\mathcal{A}_*$ has the following multipliers:

$$\lambda_1^{PD,*} = -1, \qquad \lambda_2^{PD,*} = -\frac{\delta^2 h^2 + \delta\, h^2\sigma - 3\,\delta\, h - 3\, h\sigma + 2}{\delta\, h + h\sigma - 2}.$$

The Jacobian matrix $\mathcal{A}_*^{SIR}$ has a simple eigenvalue -1 and no other eigenvalue with $|\lambda| = 1$ if $\lambda_2^{PD,*} \neq \pm 1$. So, the model (3) at $\Lambda = \Lambda_{PD,*}$ can be reduced to its normal form

$$\omega_{PD,*} \mapsto -\omega_{PD,*} + \phi_{PD,*}\omega_{PD,*}^3 + \mathcal{O}(\omega_{PD,*}^4),$$

where

$$\phi_{PD,*} = \frac{\phi_{PD,*}^1}{(\delta+\sigma)(\delta^2h^2 + \delta\, h^2\sigma - 4\,\delta\, h - 4\, h\sigma + 4)\beta^2(\delta\, h - 2)^2},$$

and

$$\phi_{PD,*}^1 = (\delta\, h + h\sigma - 2)^3(\alpha\,\delta + \alpha\,\sigma - \beta)^2\Big(\alpha\,\delta^3h^2 + 2\,\alpha\,\delta^2h^2\sigma + \alpha\,\delta\, h^2\sigma^2 - \beta\,\delta^2h^2 - \beta\,\delta\, h^2\sigma$$
$$-3\,\alpha\,\delta^2 h - 4\,\alpha\,\delta\, h\sigma - \alpha\, h\sigma^2 + 2\,\beta\,\delta\, h + \beta\, h\sigma + 2\,\alpha\,\delta + 2\,\alpha\,\sigma\Big)(\alpha\,\delta\, h + \alpha\, h\sigma - \beta\, h - 2\,\alpha).$$

An indication of the type of flip bifurcation is given by the sign of $\phi_{PD,*}$. The bifurcation is supercritical (sub-critical) if it is positive (negative). □

Theorem 6. *The critical value* $\Lambda = \Lambda_{NS,*} = \frac{\delta\,((-\delta\, h - h\sigma + 1)\alpha + \beta\, h)(\delta+\sigma)^2}{(\delta\, h + h\sigma - 1)((-\delta-\sigma)\alpha + \beta)^2}$ *causes a Neimark–Sacker bifurcation of* $\mathcal{E}_*$.

Proof. The multipliers of $\mathcal{A}_*$ for $\Lambda = \Lambda_{NS,*}$ are as follows:

$$\lambda_{1,2}^{NS,*} = \frac{\pm\, i\, h\sqrt{-\delta\,(4 + \delta\,(\delta+\sigma)h^2 + (-4\,\delta - 4\,\sigma)h)(\delta+\sigma)} - 2 - \delta\,(\delta+\sigma)h^2 + (2\,\delta + 2\,\sigma)h}{-2 + (2\,\delta + 2\,\sigma)h}.$$

There are two conjugate multipliers on the unit circle in this case. So, model (3) at $\Lambda = \Lambda_{NS,*}$ can be reduced to its normal form

$$\omega_{NS,*} \mapsto \lambda_1^{NS,*}\,\omega_{NS,*} + \iota_{NS,*}\omega_{NS,*}^2\overline{\omega_{NS,*}} + \mathcal{O}(|\omega_{NS,*}|^4).$$

In Neimark–Sacker bifurcation,

$$\upsilon_{NS,*} = \Re\Big(\lambda_2^{NS,*}\,\iota_{NS,*}\Big).$$

is the first Lyapunov coefficient. The sign of $\upsilon_{NS,*}$ indicates the Neimark–Sacker bifurcation situation. A stable (unstable, resp.) closed invariant curve occurs when $\upsilon_{NS,*} < 0$ ($\upsilon_{NS,*} > 0$), and the bifurcation is supercritical (subcritical, resp.), see [24–26]. □

4.2. Two-Parameter Bifurcations

Theorem 7. *The positive fixed point* $\mathcal{E}_*$ *undergoes a strong resonance 1:2 bifurcation in the presence of*

$$\Lambda = \Lambda_{R_2,*} = -16\,\frac{\beta\,\delta\, h + \alpha\,\delta - 4\,\beta}{(\beta\,\delta\, h^2 - 4\,\beta\, h + 4\,\alpha)^2}, \quad \sigma = \sigma_{R_2,*} = -\frac{\delta^2h^2 - 4\,\delta\, h + 4}{h(\delta\, h - 4)}.$$

Proof. The Jacobian matrix $\mathcal{A}_*$ for $\Lambda = \Lambda_{R_2,*}$ and $\sigma = \sigma_{R_2,*}$ has two multipliers $\lambda_{1,2}^{R_2,*} = -1$. So, (3) can be written as

$$\begin{pmatrix} v_{R_2,*} \\ w_{R_2,*} \end{pmatrix} \mapsto \begin{pmatrix} -v_{R_2,*} + w_{R_2,*} \\ -w_{R_2,*} + \upsilon_{R_2,*} v_{R_2,*}^3 + \gamma_{R_2,*} v_{R_2,*}^2 w_{R_2,*} \end{pmatrix},$$

where

$$\upsilon_{R_2,*} = \frac{\upsilon_{R_2}^1}{\beta^2 h^2 (\delta\, h - 4)^6}, \quad \gamma_{R_2,*} = \frac{\gamma_{R_2,*}^1}{\beta^2 h^2 (\delta\, h - 4)^6},$$

with

$$\begin{aligned}\upsilon_{R_2,*}^1 = {} & \left(\beta\,\delta\, h^2 - 4\,\beta\, h + 4\,\alpha\right)^2 \left(\beta\,\delta\, h^2 + 2\,\alpha\,\delta\, h - 4\,\beta\, h - 4\,\alpha\right)\left(\beta\,\delta^2 h^3 - 2\,\beta\,\delta\, h^2 + 8\,\alpha\,\delta\, h \right. \\ & \left. -8\,\beta\, h - 8\,\alpha\right)(\delta\, h - 2), \\ \gamma_{R_2,*}^1 = {} & \left(\beta\,\delta\, h^2 - 4\,\beta\, h + 4\,\alpha\right)^2 \left(2\,\beta^2\delta^4 h^6 + 7\,\alpha\,\beta\,\delta^4 h^5 + 8\,\alpha^2\delta^4 h^4 - 20\,\beta^2\delta^3 h^5 - 60\,\alpha\,\beta\,\delta^3 h^4 \right. \\ & - 64\,\alpha^2\delta^3 h^3 + 76\,\beta^2\delta^2 h^4 + 224\,\alpha\,\beta\,\delta^2 h^3 + 240\,\alpha^2\delta^2 h^2 - 160\,\beta^2\delta\, h^3 - 480\,\alpha\,\beta\,\delta\, h^2 \\ & \left. -384\,\alpha^2\delta\, h + 192\,\beta^2 h^2 + 384\,\alpha\,\beta\, h + 192\,\alpha^2\right).\end{aligned}$$

This bifurcation is generic provided $\upsilon_{R_2,*} \neq 0$ and $\gamma_{R_2,*} \neq -3\upsilon_{R_2,*}$. □

Theorem 8. *The positive fixed point $\mathcal{E}_*$ undergoes a strong resonance 1:3 bifurcation in the presence of*

$$\Lambda = \Lambda_{R_3,*} = -9\,\frac{\beta\,\delta\, h + \alpha\,\delta - 3\,\beta}{\left(\beta\,\delta\, h^2 - 3\,\beta\, h + 3\,\alpha\right)^2}, \quad \sigma = \sigma_{R_3,*} = -\frac{\delta^2 h^2 - 3\,\delta\, h + 3}{h(\delta\, h - 3)}.$$

Proof. The Jacobian matrix $\mathcal{A}_*$ for $\Lambda = \Lambda_{R_3,*}$ and $\sigma = \sigma_{R_3,*}$ has two multipliers $\lambda_{1,2}^{R_3,*} = -\frac{1}{2} \pm \frac{\sqrt{3}}{2}$. So, (3) can be written as

$$v_{R_3,*} \mapsto e^{\frac{\pi}{2} i} v_{R_3,*} + \upsilon_{R_3,*} v_{R_3,*}^2 \overline{v_{R_3,*}} + \gamma_{R_3,*} \overline{v_{R_3,*}}^3 + \mathcal{O}(|v_{R_3,*}|^4),$$

where

$$\upsilon_{R_3,*} = \frac{\upsilon_{R_3,*}^1}{2\,(\delta\, h - 3)^3 \beta\, h}, \quad \gamma_{R_3,*} = \frac{\gamma_{R_3,*}^1}{2\,\beta^2 h^2 (\delta\, h - 3)^6},$$

with

$$\begin{aligned}\upsilon_{R_3,*}^1 = {} & -\left(\beta\,\delta\, h^2 - 3\,\beta\, h + 3\,\alpha\right)\left(i\sqrt{3}\beta\,\delta^2 h^3 + i\sqrt{3}\alpha\,\delta^2 h^2 - 5\,i\sqrt{3}\beta\,\delta\, h^2 - \beta\,\delta^2 h^3 \right. \\ & \left. -3\,i\sqrt{3}\alpha\,\delta\, h - 3\,\alpha\,\delta^2 h^2 + 6\,i\sqrt{3}\beta\, h + 3\,\beta\,\delta\, h^2 + 3\,i\sqrt{3}\alpha + 9\,\alpha\,\delta\, h - 9\,\alpha\right), \\ \gamma_{R_3,*}^1 = {} & -\left(\beta\,\delta\, h^2 - 3\,\beta\, h + 3\,\alpha\right)^2 \left(-57\,\alpha\,\beta\,\delta^3 h^4 + 144\,\alpha\,\beta\,\delta^2 h^3 - 117\,\alpha\,\beta\,\delta\, h^2 + 7\,\delta^4 \beta\, h^5 \alpha \right. \\ & - 19\,i\sqrt{3}\alpha\,\beta\,\delta^3 h^4 + 5\,i\sqrt{3}\delta^4\beta\, h^5\alpha + 45\,i\sqrt{3}\alpha\,\beta\,\delta\, h^2 - 27\,i\sqrt{3}\beta^2 h^2 - 13\,i\sqrt{3}\delta^3\beta^2 h^5 \\ & - 39\,i\sqrt{3}\alpha^2\delta^2 h^2 - 27\,i\sqrt{3}\alpha\,\beta\, h + 21\,i\sqrt{3}\beta^2\delta^2 h^4 + 9\,i\sqrt{3}\beta^2\delta\, h^3 + 54\,i\sqrt{3}\alpha^2\delta\, h \\ & + 2\,i\sqrt{3}h^6\beta^2\delta^4 + 2\,i\sqrt{3}\delta^4 h^4\alpha^2 + 6\,i\sqrt{3}\alpha^2\delta^3 h^3 - 27\,i\sqrt{3}\alpha^2 + 27\,\beta^2 h^2 + 6\,h^4\alpha^2\delta^4 \\ & + 2\,h^6\beta^2\delta^4 - 99\,\beta^2\delta\, h^3 + 75\,\beta^2\delta^2 h^4 - 21\,\beta^2\delta^3 h^5 + 63\,\alpha^2\delta^2 h^2 - 36\,\alpha^2\delta^3 h^3 + 27\,\alpha\,\beta\, h \\ & \left. -54\,\alpha^2\delta\, h + 27\,\alpha^2\right).\end{aligned}$$

As long as $v_{R_3,*} \neq 0$ and $\gamma_{R_3,*} \neq 0$, the bifurcation is generic, and the real part of $\left(\frac{3}{4}(2e^{i\frac{4\pi}{3}} v_{R_3,*} - |\gamma_{R_3,*}|^2)\right)$ confirms the invariant closed circle's stability; see [25,26]. □

Theorem 9. *The positive fixed point $\mathcal{E}_*$ undergoes a strong resonance 1:4 bifurcation in the presence of*

$$\Lambda = \Lambda_{R_4,*} = -4\,\frac{\beta\,\delta\,h + \alpha\,\delta - 2\,\beta}{(\beta\,\delta\,h^2 - 2\,\beta\,h + 2\,\alpha)^2}, \quad \sigma = \sigma_{R_4,*} = -\frac{\delta^2 h^2 - 2\,\delta\,h + 2}{(\delta\,h - 2)h}.$$

Proof. The Jacobian matrix $\mathcal{A}_*$ for $\Lambda = \Lambda_{R_4,*}$ and $\sigma = \sigma_{R_4,*}$ has two multipliers $\lambda_{1,2}^{R_4,*} = \pm\, i$. So, (3) can be written as

$$v_{R_4,*} \mapsto i\, v_{R_4,*} + v_{R_4,*} v_{R_4,*}^2 \overline{v_{R_4,*}} + \gamma_{R_4,*} \overline{v_{R_4,*}}^3 + \mathcal{O}(|v_{R_4,*}|^4),$$

where

$$v_{R_4,*} = \frac{v^1_{R_4,*}}{2\,\beta^2 h^2 (\delta\,h - 2)^6}, \quad \gamma_{R_4,*} = \frac{\gamma^1_{R_4,*}}{2\,\beta^2 h^2 (\delta\,h - 2)^6},$$

with

$$\begin{aligned} v^1_{R_4,*} = {} & -\left(\beta\,\delta\,h^2 - 2\,\beta\,h + 2\,\alpha\right)^2 \Big(6\,i\beta^2\delta^4 h^6 + 12\,i\alpha^2\delta^4 h^4 + 78\,i\beta^2\delta^2 h^4 + 28\,i\alpha^2\delta^2 h^2 \\ & + 8\,i\alpha^2\delta\,h - 62\,\alpha\,\beta\,\delta^3 h^4 + 152\,\alpha\,\beta\,\delta^2 h^3 - 152\,\alpha\,\beta\,\delta\,h^2 + 9\,\alpha\,\beta\,\delta^4 h^5 - 64\,i\alpha\,\beta\,\delta^3 h^4 \\ & - 24\,i\alpha\,\beta\,\delta\,h^2 + 48\,\alpha^2 - 36\,i\beta^2\delta^3 h^5 - 36\,i\alpha^2\delta^3 h^3 - 72\,i\beta^2\delta\,h^3 - 16\,i\alpha\,\beta\,h + 15\,i\alpha\,\beta\,\delta^4 h^5 \\ & + 84\,i\alpha\,\beta\,\delta^2 h^3 - 8\,i\alpha^2 + 24\,i\beta^2 h^2 + 72\,\beta^2\delta^2 h^4 + 48\,\alpha\,\beta\,h - 96\,\beta^2\delta\,h^3 + 152\,\alpha^2\delta^2 h^2 \\ & + 12\,\alpha^2\delta^4 h^4 - 136\,\alpha^2\delta\,h + 3\,\beta^2\delta^4 h^6 - 24\,\beta^2\delta^3 h^5 - 72\,\alpha^2\delta^3 h^3 + 48\,\beta^2 h^2\Big), \\ \gamma^1_{R_4,*} = {} & \left(\beta\,\delta\,h^2 - 2\,\beta\,h + 2\,\alpha\right)^2 \Big(4\,i\alpha^2\delta^4 h^4 + 8\,i\beta^2\delta^3 h^5 + 40\,i\alpha^2\delta^2 h^2 + 32\,i\beta^2\delta\,h^3 \\ & - 38\,\alpha\,\beta\,\delta^3 h^4 + 80\,\alpha\,\beta\,\delta^2 h^3 - 80\,\alpha\,\beta\,\delta\,h^2 + 7\,\alpha\,\beta\,\delta^4 h^5 - 16\,i\beta^2 h^2 + 26\,\beta^2\delta^2 h^4 \\ & - 24\,\alpha^2\delta\,h - 16\,\alpha^2\delta^3 h^3 - 24\,\beta^2\delta\,h^3 + 28\,\alpha^2\delta^2 h^2 - 12\,\beta^2\delta^3 h^5 + 32\,\alpha\,\beta\,h + 2\,\beta^2\delta^4 h^6 \\ & + 4\,\alpha^2\delta^4 h^4 - 4\,i\alpha\,\beta\,\delta^3 h^4 + 8\,\alpha^2 + 8\,\beta^2 h^2 + 16\,i\alpha^2 + 4\,i\alpha\,\beta\,\delta^2 h^3 + i\alpha\,\beta\,\delta^4 h^5 - i\beta^2\delta^4 h^6 \\ & - 20\,i\alpha^2\delta^3 h^3 - 24\,i\beta^2\delta^2 h^4 - 40\,i\alpha^2\delta\,h\Big). \end{aligned}$$

A generic bifurcation occurs if $\sigma_{R_4,*} \neq 0$ and $\gamma_{R_4,*} \neq 0$ and $\Pi_{R_4,*} = -\frac{i v_{R_4,*}}{|\gamma_{R_4,*}|}$ determines the bifurcation scenario near R_4 point. There are two branches of fold curves emanating from the R_4 point if $|\Pi_{R_4,*}| > 1$. □

5. Continuation Method

The numerical bifurcation analysis is performed using the MATLAB package MATCONTM; see [27].

5.1. Numerical Continuation of $\mathcal{E}_0$

Taking into account the following fixed parameters which will lead to a numerical continuation of $\mathcal{E}_0$:

$$\alpha = 0.1, \quad \beta = 0.25, \delta = 0.3, \quad \sigma = 0.4, \quad h = 1.75.$$

We consider Λ as a bifurcation parameter.

By varying Λ, the flip bifurcation occurs at $\mathcal{E}_0$ for $\Lambda = 0.040541$ where $\phi_{PD,0} = -5.448258 \times 10^{-2}$. The sign of $\phi_{PD,0}$ determines the sub-critical flip bifurcation. The stability region of $\mathcal{E}_0$ near $\mathcal{E}_0$ is presented in Figure 1.

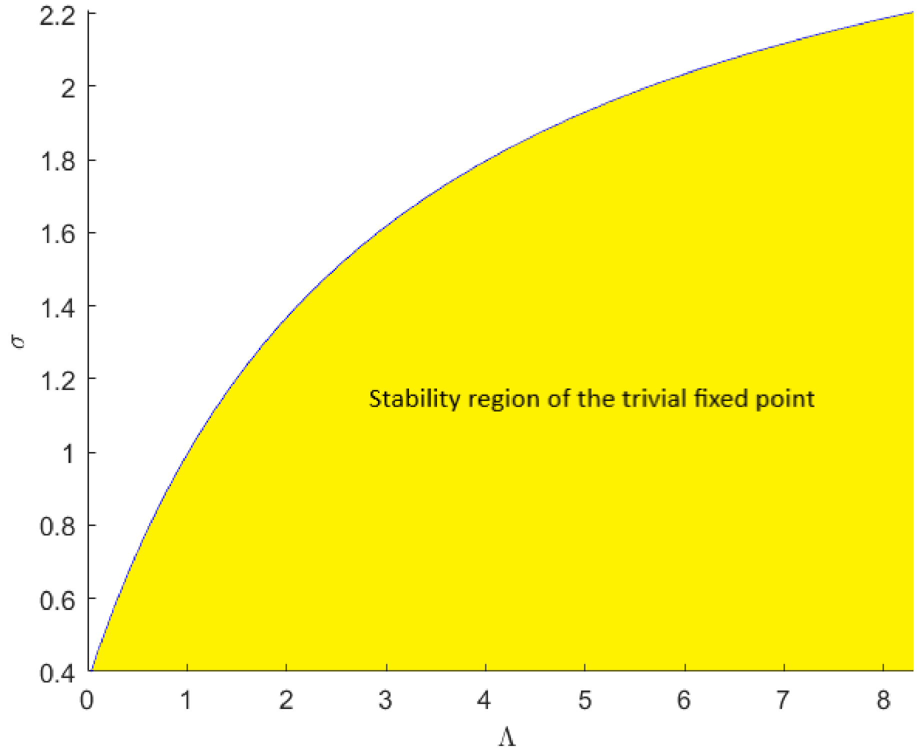

Figure 1. The stability region of $\mathcal{E}_0$ in space (Λ, σ).

5.2. Numerical Continuation of $\mathcal{E}_*$

Taking into account the following fixed parameters which will lead to a numerical continuation of $\mathcal{E}_*$:

$$\alpha = 0.01, \quad \beta = 0.25, \quad \delta = 0.3, \quad \sigma = 0.47, \quad h = 1.75.$$

We consider Λ as a bifurcation parameter.

By varying Λ, we can obtain the following one-parameter bifurcations:

1. The Neimark–Sacker bifurcation occurs at $\mathcal{E}_*$ for $\Lambda = 3.784041$ where $v_{NS,*} = 4.619653 \times 10^{-3}$. The signs of $v_{NS,*}$ determines the sub-critical Neimark–Sacker bifurcation. The phase portraits of model (3) near the Neimark–Sacker point are presented in Figure 2,
2. The flip bifurcation occurs at $\mathcal{E}_*$ for $\Lambda = 9.424221$ where $\phi_{PD,*} = -2.48869 \times 10^{-2}$. The signs of $\phi_{PD,*}$ determines the sub-critical flip bifurcation. We describe some intriguing phenomena that arise from the flip point. A bifurcation diagram of model (3) is shown in Figure 3.

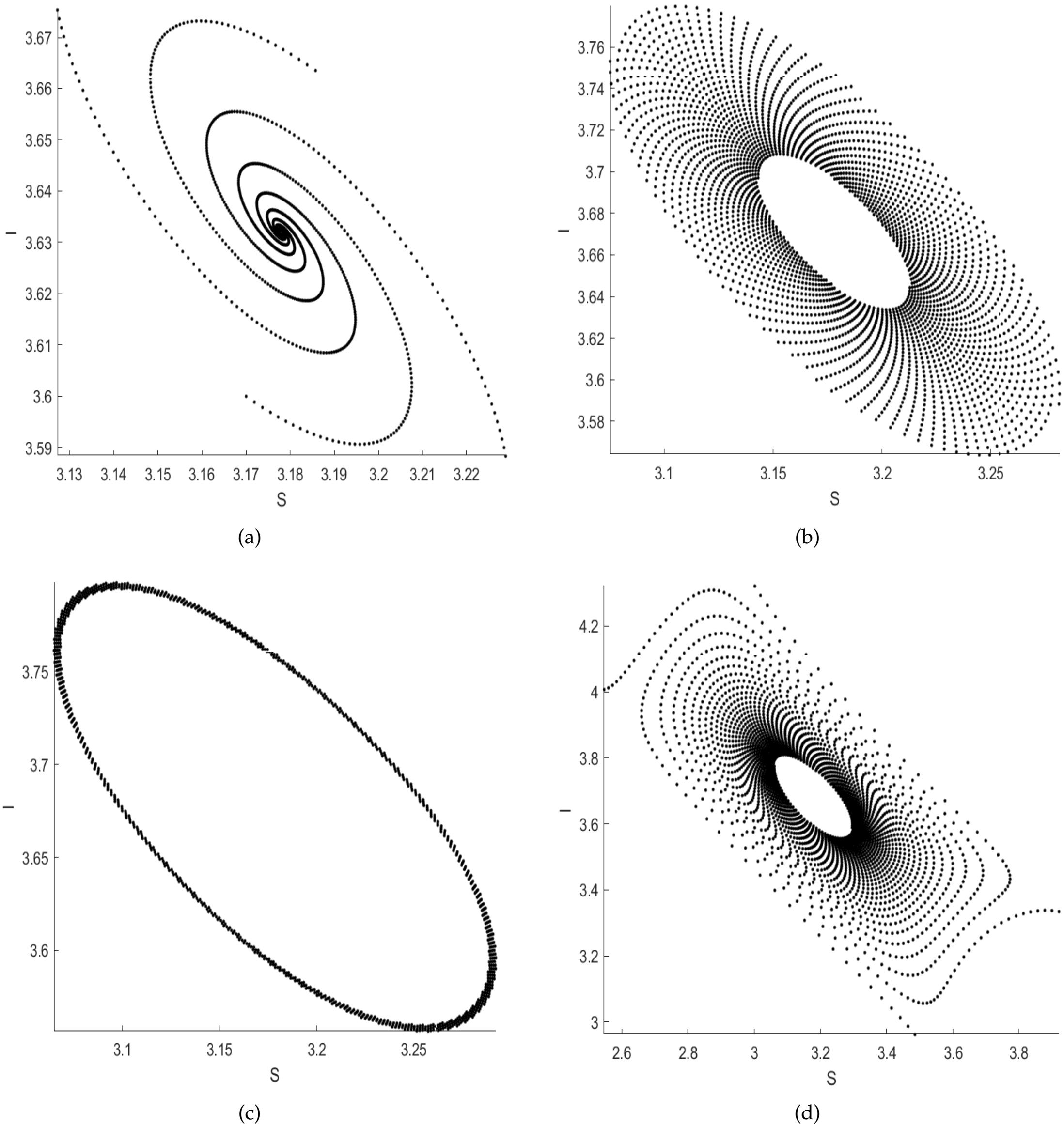

Figure 2. Phase portraits of model (3). (**a**) A stable fixed point for $\Lambda = 3.75$. (**b**) The phase portrait of model (3) for $\Lambda = 3.780$ (**c**) A closed invariant curve for $\Lambda = 3.78404$. (**d**) The broken invariant closed curve for $\Lambda = 3.788$.

The following bifurcations can be obtained with two parameters, based on the selected the Neimark–Sacker point and the continuation with two free parameters (Λ, σ):

1. The resonance 1:4 bifurcation occurs at $\mathcal{E}_*$ for $\Lambda = 3.741538$ and $\sigma = 0.474818$ where $\Pi_{R_4,*} = 9.557396 \times 10^{-2} - 2.715659 \times 10^{-1}\, i$. If we compute the convergent orbits from initial point $(S, I) = (3.1984, 3.5905)$ with respect to Λ and σ, a two-dimensional bifurcation diagram in the neighborhood of the R4 point can be displayed with the period number of the corresponding orbits [28,29]; see Figure 4. In addition to the parameter region with a period-4 cycle, there also exist regions with fixed points—period-2, -11, -15, -17, -19 and -21 cycles—to show complex periodic dynamics. Here, a stable period-4 cycle occurs when $(\Lambda, \sigma) = (3.75, 0.45)$ and one of a period-4 cycle is (3.092783505154633,3.762886597938157).
2. The resonance 1:3 bifurcation occurs at $\mathcal{E}_*$ for $\Lambda = 4.999711$ and $\sigma = 0.392641$ where $\Re\left(\frac{3}{4}(2e^{i\frac{4\pi}{3}} v_{R_3,*} - |\gamma_{R_3,*}|^2)\right) = 4.403109 \times 10^{-2}$. If we compute the convergent orbits from initial point $(S, I) = (2.8495, 5.9841)$ with respect to Λ and σ, a two-dimensional

bifurcation diagram in the neighborhood of the R3 point can be displayed with the period number of the corresponding orbits; see Figure 5. In addition to the parameter region with a period-3 cycle, there only exist regions with fixed points and a period-2 cycle. Here, a stable period-3 cycle occurs when $(\Lambda, \sigma) = (4.9, 0.38)$ and one of the period-3 cycle is (2.796052631578960,5.972329721362207).

3. The resonance 1:2 bifurcation occurs at $\mathcal{E}_*$ for $\Lambda = 6.321289$ and $\sigma = 0.357760$ where $v_{R_2,*} = -1.731233 \times 10^{-1}$ and $\gamma_{R_2,*} = 1.575539 \times 10^{-2}$. If we compute the convergent orbits from initial point $(S, I) = (2.7021, 8.3779)$ with respect to Λ and σ, a two-dimensional bifurcation diagram in the neighborhood of the R2 point can be displayed with the period number of the corresponding orbits; see Figure 6. In addition to the parameter region with a period-2 cycle, there only exist regions with fixed points and period-4, -6, and -8 cycles. Here, a stable period-2 cycle occurs when $(\Lambda, \sigma) = (5.6, 0.32)$ and one of the period-2 cycles is (2.232027014018290, 8.330641606985276); see Figure 7.

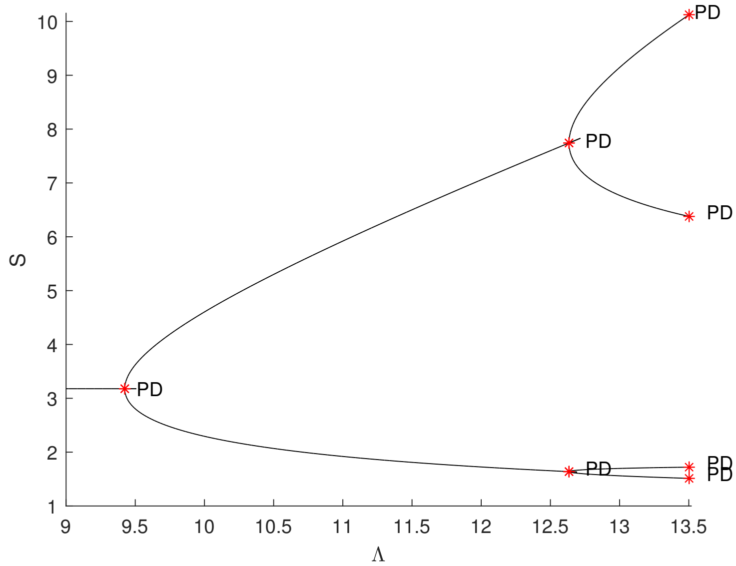

Figure 3. Bifurcation diagram of model (3) in (Λ, S)-plane.

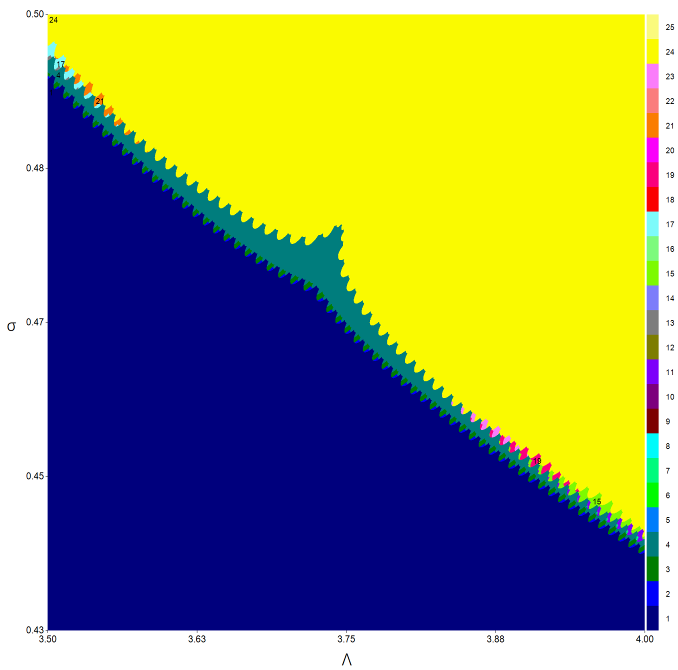

Figure 4. Two-dimensional bifurcation diagram of (3) in the neighborhood of the $R4$ point.

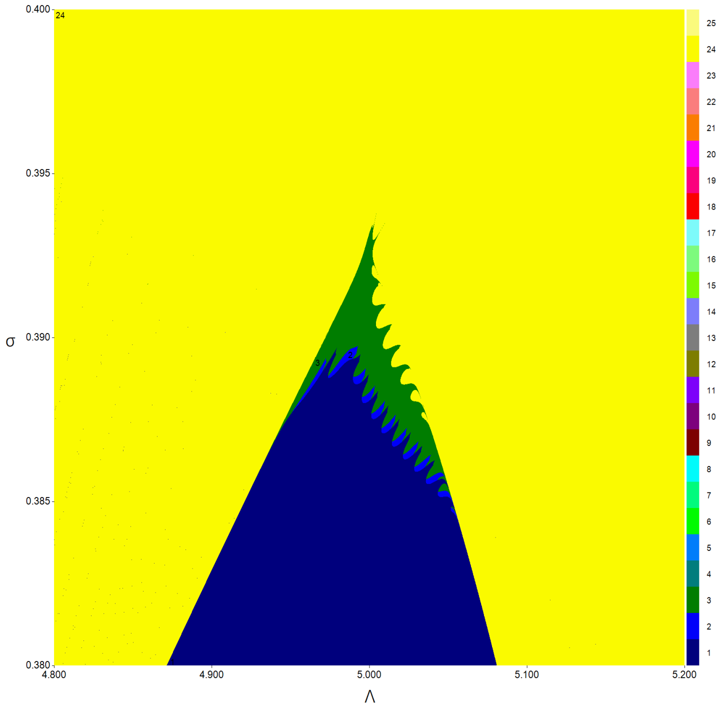

Figure 5. Two-dimensional bifurcation diagram of (3) in the neighborhood of the $R3$ point.

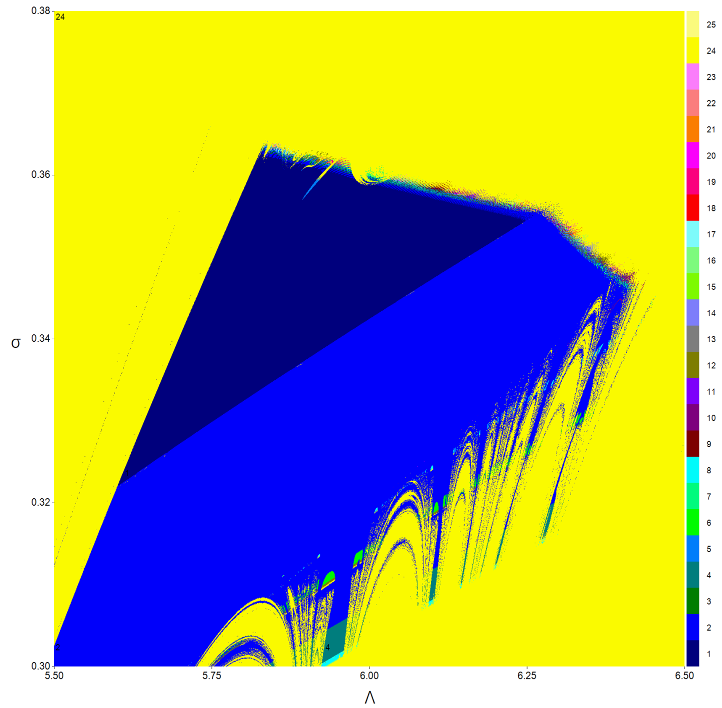

Figure 6. Two-dimensional bifurcation diagram of (3) in the neighborhood of the $R2$ point.

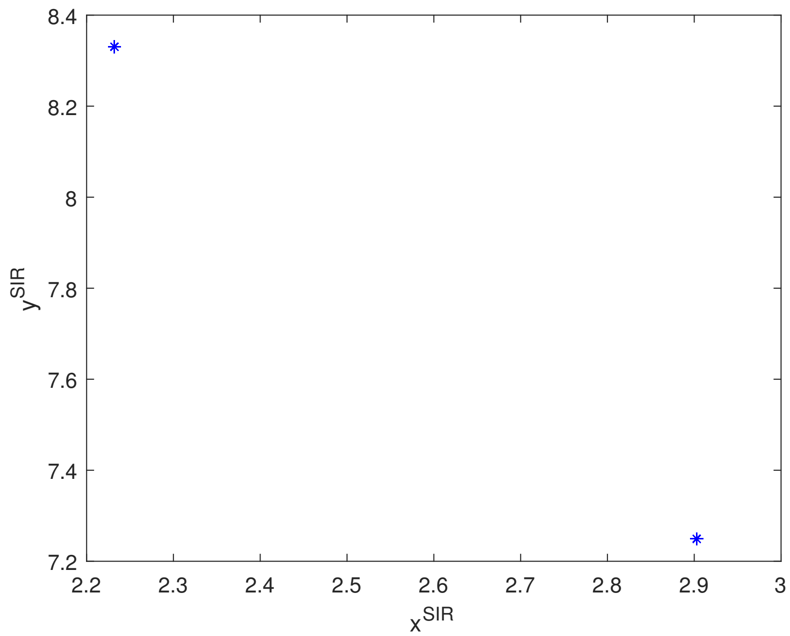

Figure 7. Stable period-2 cycle.

The stability region of $\mathcal{E}_*$ in space (Λ, σ) and the bifurcation curves of the flip and the Neimark–Sacker are shown in Figures 8 and 9. Figure 9 confirms the results of Theorems 7–9.

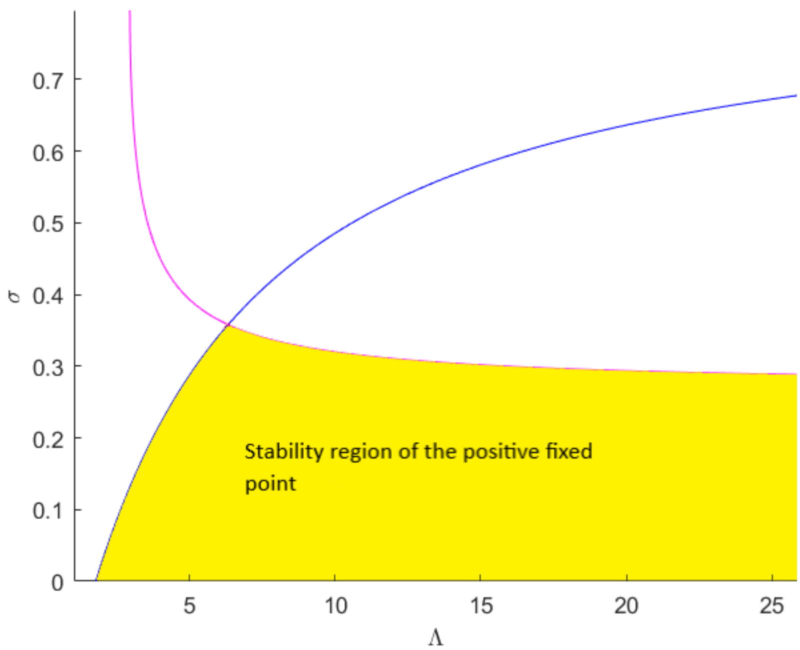

Figure 8. The stability region of $\mathcal{E}_*$ in space (Λ, σ).

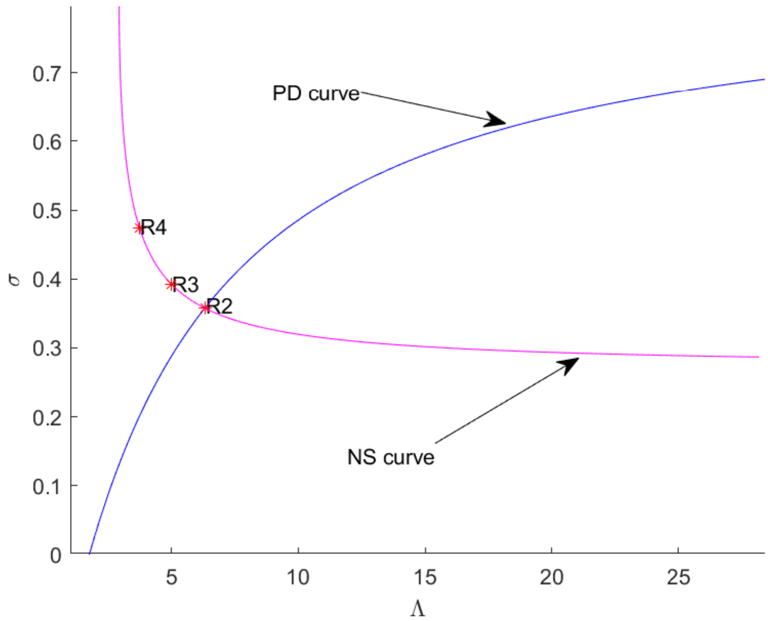

Figure 9. The bifurcation diagram of (3) near $\mathcal{E}_*$.

The bifurcation curves of the second and third iterates of (3) are presented in Figure 10a,b.

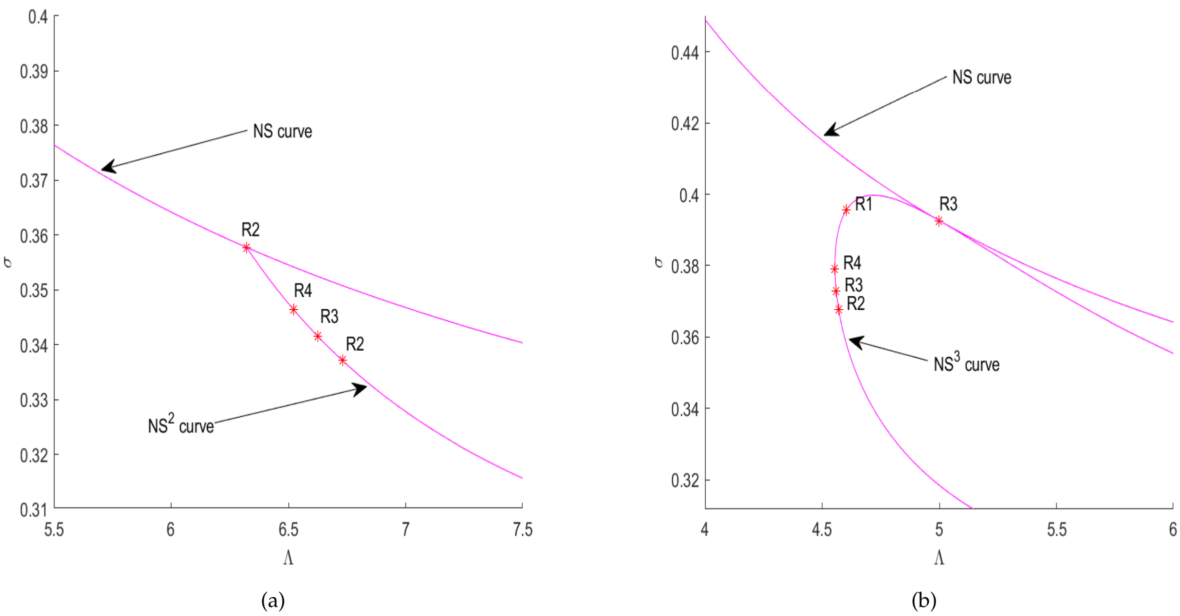

Figure 10. (**a**) The NS^2 curve. (**b**) The NS^3 curve.

6. Discussion

We presented a discrete-time SIR epidemic model with detailed complex dynamics in this study. Using analytical and numerical methods, we analyzed the bifurcation of the boundary and positive fixed points $\mathcal{E}_0^{SIR}$ and $\mathcal{E}_*^{SIR}$.

By incorporating the Neimark–Sacker bifurcation into the model, we can infer that susceptible and infective individuals can fluctuate around some mean values of the population recruitment rate, and these fluctuations remain stable as well as constant if $v_{NS,*} < 0$. According to biological theory, an invariant curve bifurcates from a fixed point, which allows susceptible and infected individuals to coexist and produce their densities. Periodic or quasi-periodic dynamics may be observed on an invariant curve. It appears that the susceptible and infected individuals change from one period to the next in this model based upon the period-doubling bifurcation. On the other hand, the strong resonances bifurcation of the model suggests susceptible and infected individuals coexist in stable high period cycles around some mean values of the rate of population recruitment rate and infection rate of infected individuals. Some two-dimensional bifurcation diagrams in the neighborhood of two-parameter bifurcation point are computed and displayed to show possible periodic dynamics.

7. Conclusions

The dynamics of a system can be identified and predicted using bifurcation theory. In this sense, bifurcation theory is an important branch of dynamical systems theory. In this paper, we provide a standard research format of bifurcation analysis. The existence and stability of fixed points are provided in Section 2. In Sections 3 and 4, one-parameter bifurcations and two-parameter bifurcations are analyzed, respectively. Detailed instructions are given in Section 5 regarding the computation of fixed point curves. According to Sections 3–5, the numerical observations and the analytical predictions are in excellent agreement. Discussions are summarized in Section 6. Both analytical and numerical aspects of bifurcations are considered in dynamic models. Some methods are more efficient than others for studying bifurcations in each of these two aspects. The computation of the critical normal form coefficients is a very effective analytical method in bifurcation theory. One can see different kinds of methods employed in bifurcation analysis [30–36]. There are many dynamical systems that are prone to notice this method, discrete or continuous; see [37–43]. An analytical computation is performed in this paper, and the results are also validated numerically using MatcontM. More details can be found in Kuznetsov and Meijer (2005) [25] and Govaerts et al. (2007) [27]. The paper also provides a robust analytical and numerical method that can be applied to different discrete-time models.

Author Contributions: Conceptualization, Z.E.; methodology, Z.E. and B.L.; software, Z.E. and B.L.; validation, B.L., Z.E. and Z.A.; formal analysis, Z.E. and B.L.; investigation, B.L., Z.E. and Z.A.; resources, Z.A.; data cu-ration, Z.E.; writing—original draft preparation, Z.E.; writing—review and editing, Z.E. and B.L.; visualization, B.L.; supervision, Z.A.; project administration, Z.A.; funding acquisition, B.L. All authors have read and agreed to the published version of the manuscript.

Funding: This work was funded by by Natural Science Foundation of Anhui Province of China (Grant No. 2008085QA09) and Scientific Research Foundation of Education Department of Anhui Province of China (Grant No. KJ2021A0482).

Informed Consent Statement: Not applicable.

Data Availability Statement: Not applicable

Acknowledgments: The authors express their sincere thanks to three referees for careful reading and valuable suggestions.

Conflicts of Interest: The authors declare no conflict of interest.

Appendix A

$$
\begin{aligned}
\Delta_*^1 = {} & -4\Lambda^2\alpha^4\delta^6h^4 - 24\Lambda^2\alpha^4\delta^5h^4\sigma - 60\Lambda^2\alpha^4\delta^4h^4\sigma^2 - 80\Lambda^2\alpha^4\delta^3h^4\sigma^3 - 60\Lambda^2\alpha^4\delta^2h^4\sigma^4 \\
& - 24\Lambda^2\alpha^4\delta h^4\sigma^5 - 4\Lambda^2\alpha^4h^4\sigma^6 + 16\Lambda^2\alpha^3\beta\delta^5h^4 + 80\Lambda^2\alpha^3\beta\delta^4h^4\sigma + 160\Lambda^2\alpha^3\beta\delta^3h^4\sigma^2 \\
& + 160\Lambda^2\alpha^3\beta\delta^2h^4\sigma^3 + 80\Lambda^2\alpha^3\beta\delta h^4\sigma^4 + 16\Lambda^2\alpha^3\beta h^4\sigma^5 - 8\Lambda\alpha^3\delta^7h^4 - 48\Lambda\alpha^3\delta^6h^4\sigma \\
& - 120\Lambda\alpha^3\delta^5h^4\sigma^2 - 160\Lambda\alpha^3\delta^4h^4\sigma^3 - 120\Lambda\alpha^3\delta^3h^4\sigma^4 - 48\Lambda\alpha^3\delta^2h^4\sigma^5 - 8\Lambda\alpha^3\delta h^4\sigma^6 \\
& + 8\Lambda^2\alpha^4\delta^5h^3 + 40\Lambda^2\alpha^4\delta^4h^3\sigma + 80\Lambda^2\alpha^4\delta^3h^3\sigma^2 + 80\Lambda^2\alpha^4\delta^2h^3\sigma^3 + 40\Lambda^2\alpha^4\delta h^3\sigma^4 \\
& + 8\Lambda^2\alpha^4h^3\sigma^5 - 24\Lambda^2\alpha^2\beta^2\delta^4h^4 - 96\Lambda^2\alpha^2\beta^2\delta^3h^4\sigma - 144\Lambda^2\alpha^2\beta^2\delta^2h^4\sigma^2 - 96\Lambda^2\alpha^2\beta^2\delta h^4\sigma^3 \\
& - 24\Lambda^2\alpha^2\beta^2h^4\sigma^4 + 24\Lambda\alpha^2\beta\delta^6h^4 + 120\Lambda\alpha^2\beta\delta^5h^4\sigma + 240\Lambda\alpha^2\beta\delta^4h^4\sigma^2 + 240\Lambda\alpha^2\beta\delta^3h^4\sigma^3 \\
& + 120\Lambda\alpha^2\beta\delta^2h^4\sigma^4 + 24\Lambda\alpha^2\beta\delta h^4\sigma^5 - 4\alpha^2\delta^8h^4 - 24\alpha^2\delta^7h^4\sigma - 60\alpha^2\delta^6h^4\sigma^2 - 80\alpha^2\delta^5h^4\sigma^3 \\
& - 60\alpha^2\delta^4h^4\sigma^4 - 24\alpha^2\delta^3h^4\sigma^5 - 4\alpha^2\delta^2h^4\sigma^6 - 32\Lambda^2\alpha^3\beta\delta^4h^3 - 128\Lambda^2\alpha^3\beta\delta^3h^3\sigma \\
& - 192\Lambda^2\alpha^3\beta\delta^2h^3\sigma^2 - 128\Lambda^2\alpha^3\beta\delta h^3\sigma^3 - 32\Lambda^2\alpha^3\beta h^3\sigma^4 + 16\Lambda^2\alpha\beta^3\delta^3h^4 + 48\Lambda^2\alpha\beta^3\delta^2h^4\sigma \\
& + 48\Lambda^2\alpha\beta^3\delta h^4\sigma^2 + 16\Lambda^2\alpha\beta^3h^4\sigma^3 + 16\Lambda\alpha^3\delta^6h^3 + 80\Lambda\alpha^3\delta^5h^3\sigma + 160\Lambda\alpha^3\delta^4h^3\sigma^2 \\
& + 160\Lambda\alpha^3\delta^3h^3\sigma^3 + 80\Lambda\alpha^3\delta^2h^3\sigma^4 + 16\Lambda\alpha^3\delta h^3\sigma^5 - 24\Lambda\alpha\beta^2\delta^5h^4 - 96\Lambda\alpha\beta^2\delta^4h^4\sigma \\
& - 144\Lambda\alpha\beta^2\delta^3h^4\sigma^2 - 96\Lambda\alpha\beta^2\delta^2h^4\sigma^3 - 24\Lambda\alpha\beta^2\delta h^4\sigma^4 + 8\alpha\beta\delta^7h^4 + 40\alpha\beta\delta^6h^4\sigma \\
& + 80\alpha\beta\delta^5h^4\sigma^2 + 80\alpha\beta\delta^4h^4\sigma^3 + 40\alpha\beta\delta^3h^4\sigma^4 + 8\alpha\beta\delta^2h^4\sigma^5 - 4\Lambda^2\alpha^4\delta^4h^2 - 16\Lambda^2\alpha^4\delta^3h^2\sigma \\
& - 24\Lambda^2\alpha^4\delta^2h^2\sigma^2 - 16\Lambda^2\alpha^4\delta h^2\sigma^3 - 4\Lambda^2\alpha^4h^2\sigma^4 + 48\Lambda^2\alpha^2\beta^2\delta^3h^3 + 144\Lambda^2\alpha^2\beta^2\delta^2h^3\sigma \\
& + 144\Lambda^2\alpha^2\beta^2\delta h^3\sigma^2 + 48\Lambda^2\alpha^2\beta^2h^3\sigma^3 - 4\Lambda^2\beta^4\delta^2h^4 - 8\Lambda^2\beta^4\delta h^4\sigma - 4\Lambda^2\beta^4h^4\sigma^2 \\
& - 40\Lambda\alpha^2\beta\delta^5h^3 - 160\Lambda\alpha^2\beta\delta^4h^3\sigma - 240\Lambda\alpha^2\beta\delta^3h^3\sigma^2 - 160\Lambda\alpha^2\beta\delta^2h^3\sigma^3 - 40\Lambda\alpha^2\beta\delta h^3\sigma^4 \\
& + 8\Lambda\beta^3\delta^4h^4 + 24\Lambda\beta^3\delta^3h^4\sigma + 24\Lambda\beta^3\delta^2h^4\sigma^2 + 8\Lambda\beta^3\delta h^4\sigma^3 + 8\alpha^2\delta^7h^3 + 40\alpha^2\delta^6h^3\sigma \\
& + 80\alpha^2\delta^5h^3\sigma^2 + 80\alpha^2\delta^4h^3\sigma^3 + 40\alpha^2\delta^3h^3\sigma^4 + 8\alpha^2\delta^2h^3\sigma^5 - 4\beta^2\delta^6h^4 - 16\beta^2\delta^5h^4\sigma \\
& - 24\beta^2\delta^4h^4\sigma^2 - 16\beta^2\delta^3h^4\sigma^3 - 4\beta^2\delta^2h^4\sigma^4 + 16\Lambda^2\alpha^3\beta\delta^3h^2 + 48\Lambda^2\alpha^3\beta\delta^2h^2\sigma \\
& + 48\Lambda^2\alpha^3\beta\delta h^2\sigma^2 + 16\Lambda^2\alpha^3\beta h^2\sigma^3 - 32\Lambda^2\alpha\beta^3\delta^2h^3 - 64\Lambda^2\alpha\beta^3\delta h^3\sigma - 32\Lambda^2\alpha\beta^3h^3\sigma^2 \\
& - 8\Lambda\alpha^3\delta^5h^2 - 32\Lambda\alpha^3\delta^4h^2\sigma - 48\Lambda\alpha^3\delta^3h^2\sigma^2 - 32\Lambda\alpha^3\delta^2h^2\sigma^3 - 8\Lambda\alpha^3\delta h^2\sigma^4 + 32\Lambda\alpha\beta^2\delta^4h^3 \\
& + 96\Lambda\alpha\beta^2\delta^3h^3\sigma + 96\Lambda\alpha\beta^2\delta^2h^3\sigma^2 + 32\Lambda\alpha\beta^2\delta h^3\sigma^3 - 8\alpha\beta\delta^6h^3 - 32\alpha\beta\delta^5h^3\sigma \\
& - 48\alpha\beta\delta^4h^3\sigma^2 - 32\alpha\beta\delta^3h^3\sigma^3 - 8\alpha\beta\delta^2h^3\sigma^4 - 24\Lambda^2\alpha^2\beta^2\delta^2h^2 - 48\Lambda^2\alpha^2\beta^2\delta h^2\sigma \\
& - 24\Lambda^2\alpha^2\beta^2h^2\sigma^2 + 8\Lambda^2\beta^4\delta h^3 + 8\Lambda^2\beta^4h^3\sigma + 8\Lambda\alpha^2\beta\delta^4h^2 + 16\Lambda\alpha^2\beta\delta^3h^2\sigma - 16\Lambda\alpha^2\beta\delta h^2\sigma^3 \\
& - 8\Lambda\alpha^2\beta h^2\sigma^4 - 8\Lambda\beta^3\delta^3h^3 - 16\Lambda\beta^3\delta^2h^3\sigma - 8\Lambda\beta^3\delta h^3\sigma^2 - 4\alpha^2\delta^6h^2 - 16\alpha^2\delta^5h^2\sigma \\
& - 24\alpha^2\delta^4h^2\sigma^2 - 16\alpha^2\delta^3h^2\sigma^3 - 4\alpha^2\delta^2h^2\sigma^4 + 16\Lambda^2\alpha\beta^3\delta h^2 + 16\Lambda^2\alpha\beta^3h^2\sigma + 8\Lambda\alpha\beta^2\delta^3h^2 \\
& + 32\Lambda\alpha\beta^2\delta^2h^2\sigma + 40\Lambda\alpha\beta^2\delta h^2\sigma^2 + 16\Lambda\alpha\beta^2h^2\sigma^3 - 8\alpha\beta\delta^5h^2 - 32\alpha\beta\delta^4h^2\sigma - 48\alpha\beta\delta^3h^2\sigma^2 \\
& - 32\alpha\beta\delta^2h^2\sigma^3 - 8\alpha\beta\delta h^2\sigma^4 - 4\Lambda^2\beta^4h^2 + 7\Lambda\alpha^2\beta\delta^3h + 21\Lambda\alpha^2\beta\delta^2h\sigma + 21\Lambda\alpha^2\beta\delta h\sigma^2 \\
& + 7\Lambda\alpha^2\beta h\sigma^3 - 8\Lambda\beta^3\delta^2h^2 - 16\Lambda\beta^3\delta h^2\sigma - 8\Lambda\beta^3h^2\sigma^2 + 8\beta^2\delta^4h^2 + 24\beta^2\delta^3h^2\sigma + 24\beta^2\delta^2h^2\sigma^2 \\
& + 8\beta^2\delta h^2\sigma^3 - 14\Lambda\alpha\beta^2\delta^2h - 28\Lambda\alpha\beta^2\delta h\sigma - 14\Lambda\alpha\beta^2h\sigma^2 + 7\alpha\beta\delta^4h + 21\alpha\beta\delta^3h\sigma \\
& + 21\alpha\beta\delta^2h\sigma^2 + 7\alpha\beta\delta h\sigma^3 + 7\Lambda\beta^3\delta h + 7\Lambda\beta^3h\sigma - 2\beta^2\delta^2 - 4\beta^2\delta\sigma - 2\beta^2\sigma^2.
\end{aligned}
$$

References

1. Barrientos, P.G. Rodríguez, J.Á.; Ruiz-Herrera, A. Chaotic dynamics in the seasonally forced SIR epidemic model. *J. Math. Biol.* **2017**, *75*, 1655–1668. [CrossRef] [PubMed]
2. Diedrichs, D.R.; Isihara, P.A.; Buursma, D.D. The schedule effect:can recurrent peak infections be reduced without vaccines, quarantines or school closings? *Math. Biosci.* **2014**, *248*, 46–53. [CrossRef]
3. Axelsen, J.B.; Yaari, R.; Grenfell, B.T.; Stone, L. Multiannual forecasting of seasonal influenza dynamics reveals climatic and evolutionary drivers. *Proc. Natl. Acad. Sci. USA* **2014**, *111*, 9538–9542. [CrossRef] [PubMed]
4. Dietz, K. The incidence of infectious diseases under the influence of seasonal fluctuations. In *Mathematical Models in Medicine*; Springer: Berlin/Heidelberg, Germany, 1976; pp. 1–15.
5. Aron, J.L.; Schwartz, I.B. Seasonality and period-doubling bifurcations in an epidemic model. *J. Theor. Biol.* **1984**, *110*, 665–679. [CrossRef]
6. Eskandari, Z.; Alidousti, J. Stability and codimension 2 bifurcations of a discrete time SIR model. *J. Frankl. Inst.* **2020**, *357*, 10937–10959. [CrossRef]

7. Li, X.; Wang, W. A discrete epidemic model with stage structure. *Chaos Solitons Fractals* **2005**, *26*, 947–958. [CrossRef]
8. Naik, P.A.; Zu, J.; Ghoreishi, M. Stability analysis and approximate solution of SIR epidemic model with Crowley-Martin type functional response and Holling type-II treatment rate by using homotopy analysis method. *J. Appl. Anal. Comput.* **2020**, *10*, 1482–1515.
9. Stone, L.; Olinky, R.; Huppert, A. Seasonal dynamics of recurrent epidemics. *Nature* **2007**, *446*, 533–536. [CrossRef]
10. Ghori, M.B.; Naik, P.A.; Zu, J.; Eskari, Z.; Naik, M. Global dynamics and bifurcation analysis of a fractional-order SEIR epidemic model with saturation incidence rate. *Math. Methods Appl. Sci.* **2022**, *45*, 1–33. [CrossRef]
11. Karaji, P.T.; Nyamoradi, N. Analysis of a fractional SIR model with general incidence function. *Appl. Math. Lett.* **2020**, *108*, 106499. [CrossRef]
12. Naik, P.A. Global dynamics of a fractional-order SIR epidemic model with memory. *Int. J. Biomath.* **2020**, *13*, 2050071. [CrossRef]
13. Zhang, Q.; Tang, B.; Tang, S. Vaccination threshold size and backward bifurcation of SIR model with state-dependent pulse control. *J. Theor. Biol.* **2018**, *455*, 75–85. [CrossRef] [PubMed]
14. BjØrnstad, O.N.; Finkenstädt, B.F.; Grenfell, B.T. Dynamics of measles epidemics: Estimating scaling of transmission rates using a time series SIR model. *Ecol. Monogr.* **2002**, *72*, 169–184.
15. Olsen, L.F.; Schaffer, W.M. Chaos versus noisy periodicity: Alternative hypotheses for childhood epidemics. *Science* **1990**, *249*, 499–504. [CrossRef]
16. Augeraud-Véron, E.; Sari, N. Seasonal dynamics in an SIR epidemic system. *J. Math. Biol.* **2014**, *68*, 701–725.
17. Duarte, J.; Januário, C.; Martins, N.; Rogovchenko, S.; Rogovchenko, Y. Chaos analysis and explicit series solutions to the seasonally forced SIR epidemic model. *J. Math. Biol.* **2019**, *78*, 2235–2258. [CrossRef]
18. Kermack, W.O.; McKendrick, A.G. A contribution to the mathematical theory of epidemics. *Proc. R. Soc. Lond. Ser. Contain. Pap. Math. Phys. Character* **1927**, *115*, 700–721.
19. Hethcote, H.W. The mathematics of infectious diseases. *SIAM Rev.* **2000**, *42*, 599–653. [CrossRef]
20. Akrami, M.H.; Atabaigi, A. Hopf and forward bifurcation of an integer and fractional-order SIR epidemic model with logistic growth of the susceptible individuals. *J. Appl. Math. Comput.* **2020**, *64*, 615–633. [CrossRef]
21. Hu, Z.; Teng, Z.; Zhang, L. Stability and bifurcation analysis in a discrete SIR epidemic model. *Math. Comput. Simul.* **2014**, *97*, 80-93. [CrossRef]
22. Liu, X.; Xiao, D. Complex dynamic behaviors of a discrete-time predator-prey system. *Chaos Solitons Fractals* **2007**, *32*, 80–94. [CrossRef]
23. He, Z.; Lai, X. Bifurcation and chaotic behavior of a discrete-time predator-prey system. *Nonlinear Anal. Real World Appl.* **2011**, *12*, 403–417. [CrossRef]
24. Kuznetsov, Y.A. *Elements of Applied Bifurcation Theory*; Springer Science & Business Media: Berlin/Heidelberg, Germany, 2013; Volume 112.
25. Kuznetsov, Y.A.; Meijer, H.G. Numerical normal forms for codim 2 bifurcations of fixed points with at most two critical eigenvalues. *Siam J. Sci. Comput.* **2005**, *26*, 1932–1954. [CrossRef]
26. Kuznetsov, Y.A.; Meijer, H.G. *Numerical Bifurcation Analysis of Maps: From Theory to Software*; Cambridge University Press: Cambridge, UK, 2019.
27. Govaerts, W.; Ghaziani, R.K.; Kuznetsov, Y.A.; Meijer, H.G. Numerical methods for two-parameter local bifurcation analysis of maps. *Siam J. Sci. Comput.* **2007**, *29*, 2644–2667. [CrossRef]
28. Li, B.; Liang, H.J.; He, Q.Z. Multiple and generic bifurcation analysis of a discrete Hindmarsh-Rose model. *Chaos Solitons Fractals* **2021**, *146*, 110856. [CrossRef]
29. Li, B.; Liang, H.J.; Shi, L.; He, Q.Z. Complex dynamics of Kopel model with nonsymmetric response between oligopolists. *Chaos Solitons Fractals* **2022**, *156*, 111860 [CrossRef]
30. Li, X.L.; Su, L. A heterogeneous duopoly game under an isoelastic demand and diseconomies of scale. *Fractal Fract.* **2022**, *6*, 459. [CrossRef]
31. Jiang, X.W.; Chen, C.; Zhang, X.H.; Chi, M.; Yan, H. Bifurcation and chaos analysis for a discrete ecological developmental systems. *Nonlinear Dyn.* **2021**, *104*, 4671–4680. [CrossRef]
32. Rahmi, E.; Darti, I.; Suryanto, A.; Trisilowati. A Modified Leslie–Gower Model Incorporating Beddington–DeAngelis Functional Response, Double Allee Effect and Memory Effect. *Fractal Fract.* **2021**, *5*, 84. [CrossRef]
33. Li, P.; Yan, J.; Xu, C.; Gao, R.; Li, Y. Understanding Dynamics and Bifurcation Control Mechanism for a Fractional-Order Delayed Duopoly Game Model in Insurance Market. *Fractal Fract.* **2022**, *6*, 270. [CrossRef]
34. Wang, H.; Ke, G.; Pan, J.; Hu, F.; Fan, H. Multitudinous potential hidden Lorenz-like attractors coined. *Eur. Phys. J.-Spec. Top.* **2022**, *231*, 359–368. [CrossRef]
35. Wang, N.; Zhang, G.S.; Kuznetsov, N.V.; Bao, H. Hidden attractors and multistability in a modified Chua's circuit. *Commun. Nonlinear Sci. Numer. Simul.* **2021**, *92*, 105494. [CrossRef]
36. Ali, M.S.; Narayanan, G.; Shekher, V.; Alsulami, H.; Saeed, T. Dynamic stability analysis of stochastic fractional-order memristor fuzzy BAM neural networks with delay and leakage terms. *Appl. Math. Comput.* **2020**, *369*, 124896.
37. Eskandari, Z.; Alidousti, J.; Avazzadeh, Z.; Ghaziani, R.K. Dynamics and bifurcations of a discrete time neural network with self connection. *Eur. J. Control* **2022**, *66*, 100642. [CrossRef]
38. Eskandari, Z.; Alidousti, J.; Avazzadeh, Z.; Machado, J.T. Dynamics and bifurcations of a discrete-time prey-predator model with Allee effect on the prey population. *Ecol. Complex.* **2021**, *48*, 100962. [CrossRef]

39. Eskandari, Z.; Avazzadeh, Z.; Ghaziani, R.K. Complex dynamics of a Kaldor model of business cycle with discrete-time. *Chaos, Solitons Fractals* **2022**, *157*, 111863. [CrossRef]
40. Eskandari, Z.; Avazzadeh Z.; Khoshsiar Ghaziani, R.; Li, B. Dynamics and bifurcations of a discrete-time Lotka-Volterra model using non-standard finite difference discretization method. *Math. Methods Appl. Sci.* **2022**. [CrossRef]
41. Xiao, Y.; Zhang, S.G.; Peng, Y. Dynamic investigations in a Stackelberg model with differentiated products and bounded rationality. *J. Comput. Appl. Math.* **2022**, *414*, 114409. [CrossRef]
42. Barge, H.; Sanjurjo, J.M.R. Higher dimensional topology and generalized Hopf bifurcations for discrete dynamical systems. *Discret. Contin. Dyn. Syst.* **2021**, *42*, 2585–2601. [CrossRef]
43. Tassaddiq, A.; Shabbir, M.S.; Din, Q.; Naaz, H. Discretization, Bifurcation, and Control for a Class of Predator-Prey Interactions. *Fractal Fract.* **2020**, *6*, 31. [CrossRef]